# Applicability of UWB Double Directional Propagation Modeling for Evaluating UWB Transmission Performance

Katsuyuki HANEDA†, Jun-ichi TAKADA†‡, and Takehiko KOBAYASHI††
†Tokyo Institute of Technology, S6–4, 2–12–1, O-okayama, Meguro-ku, Tokyo, 152–8550 Japan
E-mail: haneda@ap.ide.titech.ac.jp
‡National Institute of Information and Communications Technology, Japan
††Tokyo Denki University, Japan

***Abstract*— This paper investigates the applicability of deterministic ultra wideband (UWB) propagation modeling for evaluating UWB system performances. The modeling explores the wave propagation characteristics on both transmitting and receiving antenna sides, which is known as the double directional modeling. In evaluating the applicability, bit error probability (BEP) performances were derived using two kinds of channel impulse responses: 1) raw data which were measured by channel sounding campaign and 2) reconstructed data from the propagation modeling results. In the BEP simulation, the direct sequence UWB system was considered. Comparison of the BEP performances from two kinds of channels revealed that the concept of the double directional modeling was capable of evaluating BEP performances accurately. However, it was also found that the limitation of our double directional modeling approach based on the model-based ray path extraction method resulted in the limited capability in modeling the total received power. As a consequence, fading statistics of the reconstructed channels were different from the measured data, ending up with less accuracy to predict BEP performances depending on the data rate. Finally, possible solutions to improve the double directional propagation modeling were suggested.**

## I. Introduction

Ultra wideband (UWB) technologies have attracted much attention due to their potential to realize high data rate transmission, low-power consumption, and high precision ranging and positioning. In designing and evaluating UWB systems, one must inevitably consider multipath channels. In most UWB transmission simulations, the multipath channels are practically generated by channel models. Here, there are two types of channel models in demand mainly by different purposes: 1) channel models for system design, and 2) channel models for assessing equipment. In the former use, channel models are used to compare performances of transmission schemes, such as modulation and coding, so that one can state the superiority of the proposed approach. Such models are referred to as standard models, which are represented by IEEE 802.15.3a/4a models [1], [2]. These models are stochastic models which express the channel behaviour based on probability theories. In contrast, testing the performances of equipment under real environments is another demand by product vendors. As that activity requires precise information about channels in which products are installed, channel models should be deterministic models.

We have conducted UWB deterministic channel sounding and propagation modeling, and analyzed propagation behaviours based on physical phenomena. The modeling included angular characteristics of wave propagation both on the transmitting (Tx) and receiving (Rx) antenna sides. This method is called "double directional channel modeling". The analysis is advantageous in two senses: 1) separation of antennas and propagation is possible, leading to the development of antenna-independent channel models [3]. We thus differentiate our modeling results from other channel models by calling it "propagation models"; and 2) identification of major scattering objects causing reflection, diffraction, and penetration can be performed (*e.g.*, [4], [5]). However, how the double directional channel sounding and propagation modeling can accurately simulate the performances of UWB systems has not yet been investigated. This paper presents a comparison of bit error probability (BEP) performances when 1) raw channel transfer function (or equivalently impulse responses), and 2) results of propagation modeling are used. Data transmission simulations using raw channel data is generally called stored channel simulations (*e.g.*, [6], [7]), while the propagation models are derived from the raw channel data.

## II. UWB Double Directional Channel Souding and Propagation Modeling

### A. Channel Sounding

The double directional UWB channel sounding campaign was conducted in a wooden house. The floor plan of the measurement environment is shown in Fig. 1. The room was almost empty except for desks and displays equipped on the wall. In Fig. 1, the position of Tx and Rx antenna are shown. Tx and Rx antennas were mounted $1.30$ and $1.00$ m respectively above the floor. We measured two scenarios with different Tx positions: Scenario I had a line-of-sight to the Rx, while Scenario II did not have a line-of-sight because the door separating the room and corridor was shut during the experiment. The Tx–Rx distance on the horizontal plane was $5.00$ and $5.59$ m in Scenarios I and II, respectively.

With the use of a vector network analyzer, we measured channel transfer functions from $3.1$ to $5.0$ GHz. Furthermore, by moving the antenna position at link ends, we obtained a spatial distribution of the channel transfer functions. On the Tx side, $4$ antenna positions which realized a synthetic linear array were used, while the Rx side realized a $4 \times 4$ rectangular

1550-2252/$25.00 ©2007 IEEE

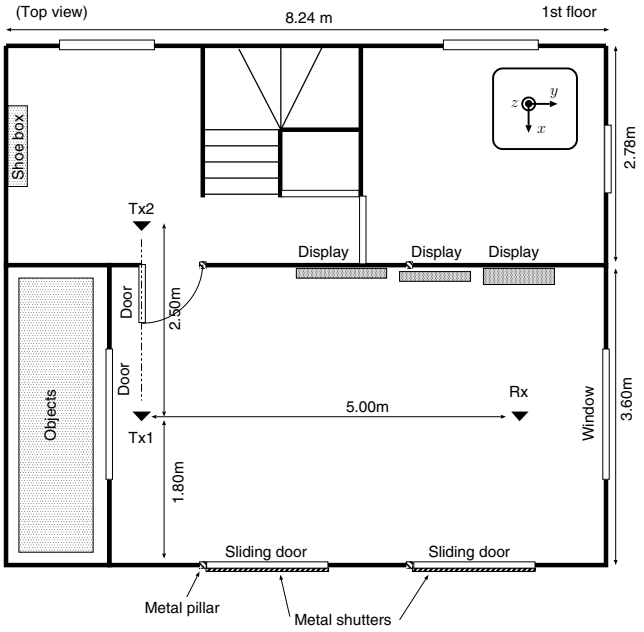


Fig. 1. Floor plan of the UWB channel sounding campaign in a home environment.

TABLE I
SPECIFICATIONS OF THE UWB DOUBLE DIRECTIONAL CHANNEL SOUNDING.

| | |
|---|---|
| Interelement spacings of the array | 48 mm on both sides of the link. |
| Antennas | UWB monopole antennas [8]. |
| Polarization | Vertical–Vertical. |
| Calibration | Internal function of VNA (port–port), Back-to-back at 1 m (antenna–antenna) |
| Signal-to-noise ratio at Rx | At least 20 dB. |

array on the horizontal plane. In total, $4 \times 4 \times 4 = 64$ spatial realizations were obtained. Other measurement specifications are summarized in Table I.

### B. Propagation Modeling

The spatial transfer function distribution was then applied to a maximum-likelihood (ML) based multi-dimensional channel parameters estimation algorithm [9]. It enables us to model radio channels in a parametric manner by characterizing the measured data as a set of discrete ray paths. Direction-of-departure (DOD), direction-of-arrival (DOA), delay time (DT), and complex gain of each discrete ray path were estimated using the algorithm.

After the parameters were estimated, directivities of the Tx and Rx antennas were compensated from the complex path gain by using obtained DOD and DOA. Tx and Rx antenna directivities were measured prior to the channel sounding in an anechoic chamber. The resultant complex path gain ideally expresses only propagation characteristics.

### C. Modeling Results

In Fig. 2, we show the power delay profile (PDP) derived from the raw channel data and reconstructed from the propagation modeling results. The PDP is defined as the ensemble average of $64$ instantaneous channel impulse responses (CIR) in an incoherent manner. In reconstructing the CIR from the propagation modeling results, we considered the same antennas as we used in the measurement. According to Fig. 2, the double directional modeling results do not reconstruct the original PDP properly. The strong multipath components appeared in the short delayed areas were modeled well, while modeling weaker paths in the long delayed areas was more difficult. This was simply due to the dynamic range of the paths over noise level. However, it was also found that paths with high signal-to-noise ratio were not always able to be detected. For example, looking at the PDP of Scenario I, PDP from the propagation modeling results failed to reconstruct the responses with DT around 26 ns. Paths in the area never appear as a peak in the PDP probably because they are hidden by sidelobes of the adjacent peaks with higher power appearing around 23 and 28 ns. The same holds for the PDP obtained from Scenario II with DT around $40$ ns. In Scenario I, the ML-based algorithm could extract $75$ % of the total received power, while it revealed an even lower value in Scenario II, $55$ %. It was observed that the more complicated the environment, the smaller the percentage of modeled power resulted [10]. This is due to the limited angular and delay resolution and the limited accuracy of underlying signal models (*e.g.*, plane wavefront model for direction finding) in the ML-based algorithm. Similar observations from channel sounding and modeling campaigns have been reported by several researchers, such as Molisch et al. [11], Thomä et al. [12], and Win and Scholtz [13], all of which utilized a model-based propagation parameter estimation. The modeled components consisted of strong paths, while the residual power was composed of many paths with weaker power.

The transmission simulation descibed in the next Section will use $64$ instantaneous CIR from the measurement, and that from the propagation modeling results. In deriving CIR, we applied a $-100$ dB threshold level to eliminate noise. Where the amplitude of the CIR was below the threshold, the value was padded with zeroes.

## III. UWB TRANSMISSION SIMULATION

We considered bi-phase DS-UWB systems which were actually implemented in [14]. The modulation used a spread sequence of $[+1 \ +1 \ +1 \ -1 \ -1 \ +1 \ -1]$, and each chip of the sequence was represented by a root-raised cosine (RRC) pulse. The RRC pulse spanned a bandwidth from $3.1$ to $5.0$ GHz, and its duration, $T_{\mathrm{d}}$, was set either to $2.4$ or $4.8$ ns. Transmitted binary data were mapped on the polarity of the spread sequences in conjunction with the differential encoding. It combats the inversion of waveform polarity due to propagation channels which degrades the BEP performance. The training sequence consisted of $1334$ symbols of "0", and was sent before sending the data stream so that the receiver was synchronized with the transmitter. To simplify the simulation conditions, channel coding was not taken into account.

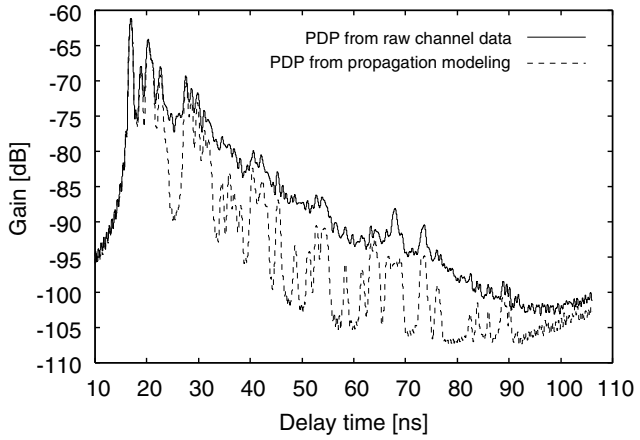


(a)

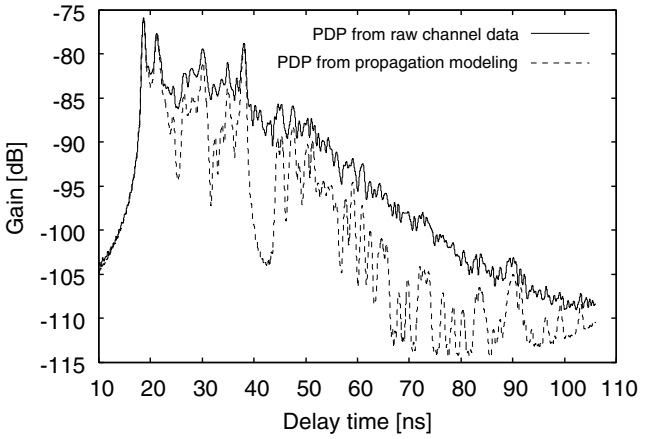


(b)

Fig. 2. PDP derived from raw channel data (solid line). PDP reconstructed from the propagation modeling results is overlayed (dashed line): (a) Scenario I and (b) Scenario II.

The simulation flow is depicted in Fig. 3. The flow emulates a structure of the testbed [14]. We assumed that signals were transmitted from the RF frontend defined at point "A" of Fig. 3 which means that characteristics of power amplifier and RF filter was compensated. The transmitted waveform was convolved with the CIR derived either from the raw data or the propagation modeling results, and then inputted to the Rx side. On the receiving side, we multiplied the receiving waveform from the Rx antennas by the transfer function of an RF filter and a low-noise amplifier (part "B" in Fig. 3) which was actually measured from the equipment. Noise level inside the receiver was also determined by that of a Digital Sampling Oscilloscope equipped on the Rx side. After the received signal was quantized by the A/D converter, the receiver demodulated signals into symbols. It correlated the received signal with a reference waveform, and identified a symbol that maximized the output. The reference waveform was the same as the transmitted one correspoding to each symbol.

## IV. Simulation Results

In this section, results of BEP simulations are described. Here we define two BEPs for the evaluation: 1) BEP obtained from $64$ spatial realizations in one scenario which we will call "local BEP", and 2) averaged BEP over the $64$ realizations which will be referred to as "average BEP".

### A. Average BEP

Figure 4 shows the average BEP characteristics dependent on energy per bit, $E_{\rm b}/N_0$, for Scenarios I and II, respectively. In each figure, two sets of curves corresponding to $T_{\rm d} = 2.4$ and $4.8$ ns are shown. Furthermore, BEP curve from stored channel simulations and propagation modeling results are shown in the same chart for comparison. As a baseline, the BEP curve assuming additive white gaussian noise (AWGN) is overlayed.

Every figure shows that the BEP is decreasing with the increase of $E_{\rm b}/N_0$ when $T_{\rm d} = 4.8$ ns. In contrast, when $T_{\rm d} = 2.4$ ns, the BEP curve reveals an error floor even when $E_{\rm b}/N_0$ increases. This is due to intersymbol interference (ISI) which tends to be more severe when the symbol length is shorter.

When comparing the BEP characteristics from the stored channel simulations and those from the propagation modeling results, the following observations were obtained:

1) In Scenario I, $T_{\rm d} = 4.8$ ns, the average BEP from propagation modeling results was always less than that of the stored channel simulations. The difference in the slope of two curves was attributed to the limited capability of the propagation modeling to extract the received power. As we discussed in Section II using the PDP, the propagation modeling successfully characterized the LOS components, while other multipath components were not properly modeled. This caused the difference of fading statistics between raw and reconstructed channels, and the average BEP from propagation modeling results approached the characteristics of AWGN channels where no multipath component existed.
2) In the results in Scenario I with $T_{\rm d} = 2.4$ ns, the average BEP curve from the stored channel simulations showed the error floor, while this was not found in the BEP from propagation modeling results. The difference was also due to the limited performances of the propagation modeling. It was found that only one out of $64$ local BEP revealed the error floor in the stored channel simulations, while all the local BEP from propagation modeling results decreased to $0$. As a result, the "nonzero" local BEP caused the difference.
3) In Scenario II, the average BEP from propagation modeling results was close to that from stored channel simulations, although the modeled power was smaller than Scenario I. This means that the modeled components had strong influence on BEP characteristics in Scenario II, while residual components had less significance. The error floor occured in $T_{\rm d} = 2.4$ ns was accurately determined. Two curves revealed irregular characteristics

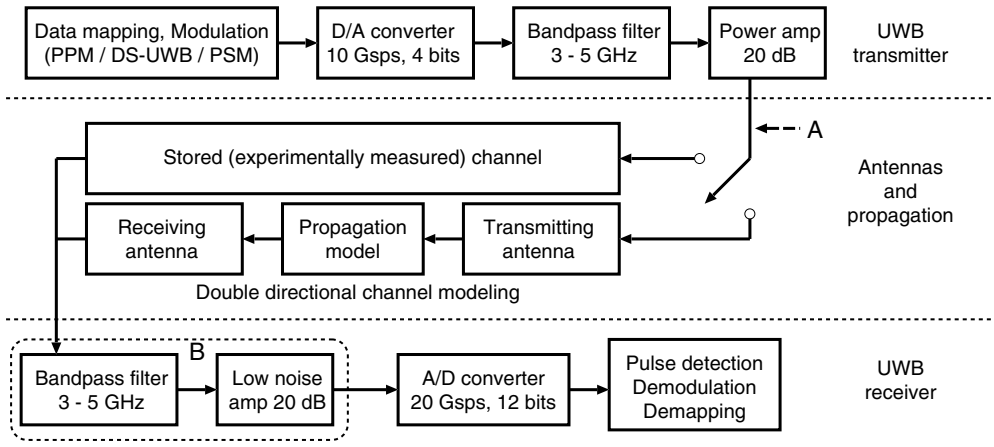


Fig. 3. Block diagram of the UWB transmission simulation using stored channels and propagation modeling results.

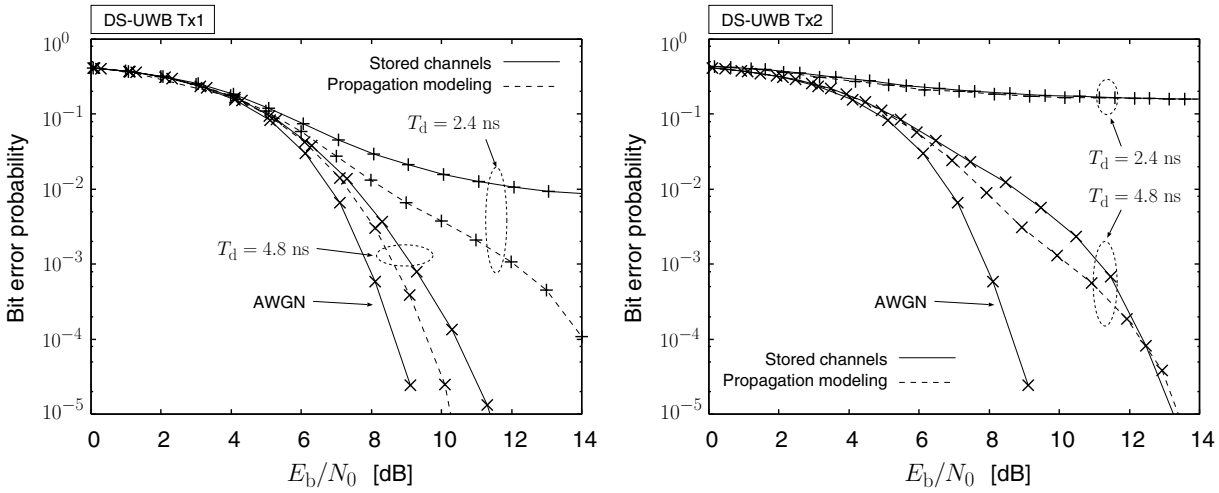


(a) (b)

Fig. 4. $E_\mathrm{b}/N_0$ versus average BEP. (a) Scenario I, (b) Scenario II.

in $T_\mathrm{d} = 4.8$ ns case, since they crossed with one another around $E_\mathrm{b}/N_0 = 12$ dB. This was due to the fluctuating slope of BEP curves, which was observed particularly when the number of spatial channel realizations was limited as our simulations (in our case, 64).

From observations 1) to 3), it was found that predicting the average BEP performances can be accurately performed using propagation modeling results when ISI oriented errors were dominant, or when the transmission data rate was sufficiently low that the system did not suffer from ISI. In contrast, differences resulted in two curves when some of the local BEP were subjected to ISI, while the others were ISI free. It is noteworthy that the same conclusion was obtained when we considered pulse position modulation systems [15].

Another important finding is that the limited capability of the propagation modeling in extracting power, *i.e.,* 75 and 55 % in Scenarios I and II respectively, affected only to the slight decrease of $E_\mathrm{b}/N_0$ compared to the stored channel simulations. The difference of $E_\mathrm{b}/N_0$ is summarized in Table II. As the degradation was at most 0.6 dB, it was again confirmed that the propagation modeling characterized multipath components that contributed to the data transmission, while the residual power had less impact.

TABLE II
DIFFERENCES OF $E_\mathrm{b}/N_0$ FOR THE TWO BEP SIMULATIONS.

| | $T_\mathrm{d} = 4.8$ ns | $T_\mathrm{d} = 2.4$ ns |
|---|---|---|
| Scenario I (LOS) | 0.2 dB | 0.1 dB |
| Scenario II (NLOS) | 0.5 dB | 0.6 dB |

### *B. Local BEP*

Next we discuss the accuracy of local BEP. Figure 5 shows the scattered plot of the local BEP derived from the stored

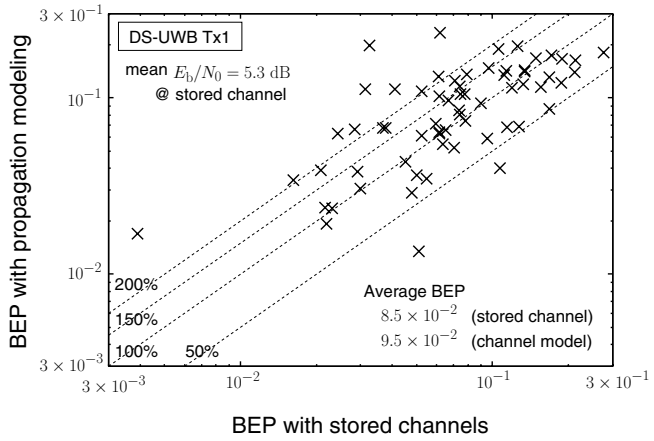


Fig. 5. Scattered plot of the local BEP using stored channels versus that from propagation modeling results. Considered channel was Tx1–Rx (Scenario I).

channel simulations and propagation modeling results. The results are from Scenario I, and mean $E_b/N_0$ of the stored channel simulations was 5.3 dB, where the average BEP was almost identical for two simulations. In the figure, there are 64 scattered points each derived from spatial realizations, which are ideally identical with each other, thus on the 100% line. In contrast to the agreement of average BEP, we can see from the figure that the local BEP from propagation modeling results did not always accurately determine the result of stored channel simulations. More than 70 % of the local BEP from propagation modeling results was within $\pm 50$ % deviation of those from stored channel simulations, but a few local BEP from propagation modeling results deviated by more than 200 or 50 % of those from stored channel simulations. The deviation stemmed from the insufficient accuracy of the propagation modeling in characterizing envelope and phase of the CIR. As the propagation modeling was performed using the multi-dimensional power angular-delay profile, which was a coherent summation of 64 CIR, the accuracy of the CIR reconstructed from propagation modeling results was not tolerable as that of the power angular-delay profile. We found that the deviation of the local BEP was much larger in Scenario II. It was also found that the deviation was more significant in high $E_b/N_0$ areas, where BEP was more sensitive to the shape of CIR.

## V. Conclusion

This paper investigated the applicability of UWB propagation modeling results for evaluating BEP performance. We considered two specific modeling examples: LOS and NLOS channels. It was found that our propagation modeling could characterize multipath components that determined average BEP, while the accuracy in predicting local BEP was worse. Even in the average BEP, the accuracy was not always enough and was dependent on the data rate. The problem lies in the model-based characterization of radio channels, and therefore, it is essential to improve the accuracy of propagation modeling, specifically by taking into account the following aspects:

1) *Modeling of the residual power.* There is a rule of thumb in modeling the residual component using the exponential decaying shape of the power delay profile [12]. However, it should be further extended to double-directional spatio-temporal domains in order to be fully integrated in the double-directional modeling strategy.
2) *Alternative approach of propagation modeling.* Non-parametric modeling (*e.g.*, [5]) and the parametric modeling with refined underlying signal models (*e.g.*, [16]) are also possible solutions.

## Acknowledgment

The authors would like to thank members of the NICT UWB Consortium for valuable helps in the experiment and discussions. This research is also partly supported by the Japan Society for the Promotion of Science Research Fellowships for Young Scientists.

## References

[1] J. Foerster *et al.* "Channel modeling sub-committee report (final)," IEEE P802.15-02/490r1-SG3a, Feb. 2003.
[2] A. F. Molisch *et al.* "IEEE 802.15.4a channel model – final report," IEEE P802.15-04/662r0-SG4a, Nov. 2004.
[3] M. Steinbauer, A. F. Molisch, and E. Bonek, "The double directional radio channel," *IEEE Antennas and Propagat. Mag.*, vol. 43, no. 4, pp. 51–63, Aug. 2001.
[4] K. Haneda, J. Takada, and T. Kobayashi, "Double directional ultra wideband channel characterization in a line-of-sight home environment," *IEICE Trans. Fundamentals*, E88–A, no. 9, pp. 2264–2271, Sep. 2005.
[5] K. Kalliola, H. Laitinen, P. Vainikainen, M. Toeltsch, J. Laurila, and E. Bonek, "3-D double-directional radio channel characterization for urban macrocellular applications," *IEEE Trans. Antennas Propagat.*, vol. 51, no. 11, pp. 3122–3133, Nov. 2003.
[6] K. Takizawa, S. Fujita, Y. Rikuta, K. Hamaguchi, and R. Kohno, "Measurement based performane evaluation of a 26 GHz band UWB communication system," in *Proc. 64th IEEE Veh. Tech. Conf.*, Montreal, Canada, Sep. 2006.
[7] J. Keignart, C. Abou-Rjeily, C. Delaveaud, and N. Daniele, "UWB SIMO channel measurements and simulations," *IEEE Trans. Microwave Theory Tech.*, vol. 54, no. 4, pp. 1812–1819, Apr. 2006.
[8] T. Taniguchi, A. Maeda, and T. Kobayashi, "Development of an omnidirectional and low-VSWR ultra wideband antenna," *Int. J. Wireless & Opt. Commun.*, vol. 3, no. 2, pp. 145–157, 2006.
[9] K. Haneda, J. Takada, and T. Kobayashi, "A parametric UWB propagation channel estimation and its performance validation in an anechoic chamber," *IEEE Trans. Microwave Theory Tech.*, vol. 54, no. 4, pp. 1802–1811, Apr. 2006.
[10] ————, "Cluster properties investigated from a series of ultra wideband double directional propagation measurements in home environments," *IEEE Trans. Antennas Propagat.*, vol. 54, no. 12, pp. 3778–3788, Dec. 2006.
[11] A. F. Molisch, M. Steinbauer, M. Toeltsch, E. Bonek, and R. S. Thomä, "Capacity of MIMO systems based on measured wireless channels," *IEEE J. Select. Areas Commun.*, vol. 20, no. 3, pp. 561–569, Apr. 2002.
[12] R. S. Thomä, M. Landmann, A. Richter, and U. Trautwein, *Multidimensional High-Resolution Channel Sounding.* in *Smart Antennas in Europe – State-of-the-Art*, EURASIP Book Series, Hindawi Publishing Corporation, New York, USA, 2005.
[13] M. Z. Win and R. A. Scholtz, "Characterization of ultra-wide bandwidth wireless indoor channels: a communication-theoretic view," *IEEE J. Select. Areas Commun.*, vol. 20, no. 9, pp. 1613–1627, Dec. 2002.
[14] K. Takizawa, H. B. Li, I. Nishiyama, J. Takada, and R. Kohno, "Overview of research, development, standardization, and regulation activities in NICT UWB Project," *IEICE Trans. Fundamentals*, vol. E89–A, no. 11, pp. 2996–3005, Nov. 2006.
[15] K. Haneda, J. Takada, and T. Kobayashi, "Applicability of UWB double directional propagation modeling for evaluating UWB transmission erformance," *IEICE Tech. Rep.*, WBS2006–27, Sendai, Japan, pp. 19–24, Oct. 2006.
[16] C. Ribeiro, A. Richter, and V. Koivunen, "Stochastic maximum likelihood estimation of angle- and delay domain propagation parameters," in *Proc. 16th Int. Symp. Personal Indoor and Mobile Radio Commun. (PIMRC '05)*, C05–05, Berlin, Germany, Sep. 2005.